

Highlights:

- Suppressing hepatic glucose-6 phosphatase prevents and cures diabetes and obesity
- Mechanisms involve increased peripheral energy expenditure and glucose oxidation
- Hepatokines fibroblast-growth factor 21 and angiopoietin-like factor 6 are a link
- Hepatic glucose metabolism regulates peripheral energy metabolism

A link between hepatic glucose production and peripheral energy metabolism *via* hepatokines

1
2
3 Aya Abdul-Wahed¹⁻⁴, Amandine Gautier-Stein¹⁻³, Sylvie Casteras¹⁻³, Maud Soty¹⁻³, Damien
4
5 Roussel^{2,3,5}, Caroline Romenstaing^{2,3,5}, Hervé Guillou⁶, Jean-André Tourette¹⁻³, Nicolas Pleche¹⁻³,
6
7 Carine Zitoun¹⁻³, Blandine Gri³, Anne Sardella¹⁻³, Fabienne Rajas¹⁻³ & Gilles Mithieux¹⁻³
8
9

10
11 ¹Institut National de la Santé et de la Recherche Médicale, U855, Lyon, F-69008, France
12
13

14 ²Université de Lyon, Lyon, F-69008 France
15

16 ³Université Lyon1, Villeurbanne, F-69622 France
17
18

19 ⁴University of Aleppo, Aleppo, Syria
20

21 ⁵Centre National de la Recherche Scientifique, UMR5023, Villeurbanne, F-69622, France
22
23

24 ⁶INRA-ToxALim, Toulouse, F-31027 France
25
26
27
28

29 **List of E-mail address:** A. Abdul-Wahed: aya_abdulwahed@hotmail.com; A. Gautier-Stein
30
31 amandine.gautier-stein@univ-lyon1.fr; S. Casteras : sylvie.casteras@gmail.com ; M. Soty :
32
33 maud.soty@gmail.com; D. Roussel : damien.roussel@univ-lyon1.fr; C. Romenstaing :
34
35 caroline.romestaing@univ-lyon1.fr; H. Guillou : Herve.Guillou@toulouse.inra.fr; JA. Tourette:
36
37 juanito.t@hotmail.fr; N. Pleche : nicolas.pleche@hotmail.fr; C. Zitoun : carine.zitoun@univ-
38
39 lyon1.fr; B. Gri : blandine.gri@hotmail.fr; A. Sardella : anne.sardella@inserm.fr ; F. Rajas :
40
41 fabienne.rajas@univ-lyon1.fr; G. Mithieux : gilles.mithieux@univ-lyon1.fr
42
43
44
45
46
47
48

49 **Corresponding author:** Dr. Gilles Mithieux, Inserm U855, Université Lyon 1 Laennec, 7 rue
50

51 Guillaume Paradin, 69372 Lyon cedex 08 France
52

53 Tel: 33 478 77 87 88/Fax: 33 478 77 87 62; E-mail: gilles.mithieux@univ-lyon1.fr
54
55
56

57 **Running head:** Hepatic glucose production and hepatokines
58
59
60
61
62
63
64
65

ABSTRACT

1 Type 2 diabetes is characterized by a deterioration of glucose tolerance, which associates insulin
2
3 resistance of glucose uptake by peripheral tissues and increased endogenous glucose production.
4
5 Here we report that the specific suppression of hepatic glucose production positively modulates
6
7 whole-body glucose and energy metabolism. We used mice deficient in liver glucose-6 phosphatase
8
9 that is mandatory for endogenous glucose production. When they were fed a high fat/high sucrose
10
11 diet, they resisted the development of diabetes and obesity due to the activation of peripheral
12
13 glucose metabolism and thermogenesis. This was linked to the secretion of hepatic hormones like
14
15 fibroblast growth factor 21 and angiopoietin-like factor 6. Interestingly, the deletion of hepatic
16
17 glucose-6 phosphatase in previously obese and **insulin-resistant** mice resulted in the rapid
18
19 restoration of glucose and body weight controls. Therefore, hepatic glucose production is an
20
21 essential lever for the control of whole-body energy metabolism during the development of obesity
22
23 and diabetes.
24
25
26
27
28
29
30
31
32

33 **KEY WORDS:** liver, endogenous glucose production, hepatokines, type 2 diabetes, obesity,
34
35 energy expenditure.
36
37
38
39
40
41
42
43
44
45
46
47
48
49
50
51
52
53
54
55
56
57
58
59
60
61
62
63
64
65

1. INTRODUCTION

In recent years, there has been an alarming increase worldwide in the prevalence of obesity and related pathologies, particularly type 2 diabetes (T2D), affecting hundreds of millions of people [1]. T2D is characterized by a deterioration of glucose control, involving abnormalities in insulin action, insulin secretion and endogenous glucose production (EGP), and resulting in increased fasting plasma glucose [2–4]. The crucial issue of knowing which of these defects is dominant in the onset of hyperglycemia and the further development of the hallmarks of diabetes is still a subject of continuous debate. For decades, diabetes research has focused on insulin resistance (IR) and decreased peripheral glucose handling, considered as the primary defect in the pathogenesis of diabetes [2]. However, mice lacking insulin receptors in both muscle and white adipose tissue (WAT) exhibited IR to glucose uptake, but failed to become diabetic [5]. This has questioned the primacy of peripheral IR in the development of T2D. On the other hand, fasting hyperglycemia in T2D patients is associated with increased EGP [6–11]. EGP is generally considered to play a major worsening role in the appearance of hyperglycemia under conditions of IR. Indeed, the two pathways accounting for EGP -glycogenolysis and gluconeogenesis- are stimulated by glucagon, while hyperglucagonemia is a hallmark of T2D [12,13].

The current paradigm generally assimilates EGP to “hepatic” glucose production (HGP). However, besides the liver, two other organs are capable of producing glucose, namely the kidney and small intestine, because they express the catalytic subunit of the glucose-6 phosphatase (G6Pase) enzyme (encoded by *G6pc*) [14]. G6Pase is the mandatory enzyme of EGP, involved in the last reaction preceding glucose release in blood. It is noteworthy that glucose production by the small intestine initiates a gut-brain neural communication with positive outcomes on glucose and body weight control [[15,16] for reviews]. The induction of small intestine gluconeogenesis notably accounts for the metabolic benefits associated to dietary protein or soluble fiber [17–19]. This has

1 urged us to re-examine the current paradigm assimilating EGP to HGP, as far as a worsening role in
2 T2D is concerned. Recently, we generated mice with a liver-specific deletion of *G6pc* (L-G6pc^{-/-}
3 mice). These exhibit the liver phenotype associated to the G6Pase deficiency, including glycogen
4 accumulation and increased lipogenesis. However, despite the fact they do not produce glucose in
5 the liver, L-G6pc^{-/-} mice are viable, exhibit **normal blood glucose level** in the fed state, and even
6 resist fasting due to the compensatory induction of intestinal and renal glucose production [20].
7
8 Therefore, L-G6pc^{-/-} mice are suitable to assess the specific role of the liver in the development of
9 T2D by feeding a high fat/high sucrose diet (HF/HS). Our hypothesis was that these mice should
10 resist diabetes. Here, we report that the specific suppression of EGP from the hepatic site protects
11 not only against T2D, but also against obesity, *via* hepatic hormonal crosstalk with peripheral
12 tissues.
13
14
15
16
17
18
19
20
21
22
23
24
25
26
27

28 **2. MATERIAL AND METHODS**

29
30 **2.1. Animals and diet.** L-G6pc^{-/-} mice were generated as described previously [21]. We used only
31 male adult B6.G6pc^{lox/lox}.SA^{CreERT2} (G6pc^{lox/lox}), L-G6pc^{-/-} and C57Bl/6J control (+/+ or wild-type,
32 Charles Rivers Laboratories, France) mice for the present studies. Mice with a double knock-out of
33 *Fgf21* and *G6pc* were obtained by crossing B6.Fgf21^{-/-} mice [22] and B6.G6pc^{lox/lox}.SA^{CreERT2}.
34
35 Progeny (6-8 weeks old) was then injected once daily with 100 µL of tamoxifen (10 mg/mL) on 5
36 consecutive days to delete the *G6pc* exon 3 in the liver. All mice were housed in the animal facility
37 of Lyon 1 University (*Animaleries Lyon Est Conventiionnelle et SPF*) under controlled temperature
38 (22°C) conditions, with a 12-hour light-12-hour dark cycle. Mice had free access to water and diet.
39
40 Fasted mice were provided with continual free access to water. HF/HS diet (consisting of 36.1% fat,
41 35% carbohydrates (50% maltodextrine+50% sucrose), 19.8% proteins) was produced by the Unité
42 de Préparation des Aliments Expérimentaux (UE0300) of the Institut National de la Recherche
43 Agronomique (INRA, UE0300, Jouy-en-Josas, France). HF/HS diet was weighed and changed 3
44
45
46
47
48
49
50
51
52
53
54
55
56
57
58
59
60
61
62
63
64
65

times a week. All procedures were performed in accordance with the principles and guidelines established by the European Convention for the Protection of Laboratory Animals. The regional animal care committee (CREEA, CNRS, Rhône Auvergne, France) approved all experiments.

2.2. Glucose and insulin tolerance tests. GTT and ITT were performed in fed state. Mice were injected with 1 g of glucose per kg body weight for GTT, and 0.75 U of insulin per kg body weight for ITT, intraperitoneally. Blood was withdrawn from the tail vein at indicated times for glucose and/ or insulin assessment. Blood glucose was measured using an “Accu-Chek Go” glucometer (Roche Diagnostics).

2.3. Body composition and basal metabolism studies. Studies were performed after 16 weeks of HF/HS feeding. Fat and lean mass was assessed by dual-energy X-ray absorptiometry (Piximis, Madison, WI). For indirect calorimetry, oxygen consumption and carbon dioxide production were determined using a single chamber system (Oxylet, Panlab-Bioseb, France). Energy expenditure was normalized with respect to body weight. Respiratory quotient was determined as the ratio of VCO_2 to VO_2 . Physical activity was measured using two level infrared beams to count the number of beam breaks during 24 hours (Bioseb, France). Body temperature was assessed using a rectal probe (Harvard Apparatus).

2.4. Determination of 2-deoxyglucose uptake. A catheter was indwelled into the right jugular vein under isoflurane anesthesia and mice were allowed to recover for 4 to 6 days. Experiments were done in the middle of the light period and food was withdrawn 1 hour before the experiment. Conscious and unrestrained mice were infused with a bolus ($3\mu\text{Ci}$) of [^{14}C]2-deoxy-D-glucose (NEN Perkin). Blood glucose was monitored using a glucometer and blood samples were collected at different time points to assess blood [^{14}C]2-deoxy-D-glucose radioactivity. One hour after the bolus, mice were euthanized with a lethal dose of pentobarbital and tissues were immediately dissected for assessment of individual tissue [^{14}C]2-deoxy-D-glucose uptake. Tissue glucose uptake

was calculated by estimation of [¹⁴C]2-deoxy-D-glucose-6 phosphate accumulation in the tissue [23].

2.5. Mitochondrial respiration. Oxygen was measured using a Clark oxygen electrode (Rack Brother LTD) placed in a glass chamber thermostatically controlled at 37°C, with constant stirring. Mitochondria isolated from muscles (0.3 mg protein/mL) were incubated in a respiratory buffer in the presence of 5 mM pyruvate and 2.5 mM malate as substrates. Phosphorylating respiration (state 3) was initiated with 500 μM ADP. Non phosphorylating respiration was initiated by addition of 1 μg/mL oligomycin and fully uncoupled respiration was obtained with 2 μM carbonyl cyanide p-trifluoromethoxyphenylhydrazone (FCCP). After addition of antimycin, 2 mM ascorbate and 500 μM N,N,N',N'tetramethyl-p-phenylenediamine (TMPD) were added and the maximal respiration rate associated with isolated cytochrome c oxidase activity recorded.

2.6. Metabolic measurements. Mice were euthanized after 6h fasting by cervical dislocation. The liver was rapidly removed and frozen using tongs previously chilled in liquid N₂. Blood was withdrawn from the retroorbital vein under isofluran anesthesia and collected in EDTA. Circulating triglycerides were assessed using Biomérieux colorimetric kit. Free fatty acid concentrations were measured using colorimetric Diasys kit. Insulin concentrations were measured using a mouse insulin Elisa kit (Chrystal Chem). Ketone bodies were assessed directly on vein blood using Optium Xceed system (Abbott). Adiponectin, leptin and FGF21 were assayed using Elisa kits from Biovendor. G6P and glycogen determination were carried out on frozen tissue homogenates [24]. G6Pase activity was determined as described previously [25].

2.7. Gene expression analysis. Total RNAs were isolated from tissues with TRIzol reagent (Invitrogen). Reverse transcription and real-time PCR were performed as described previously, using sequence-specific primers (Table S1). The mouse ribosomal protein mL19 transcript (*Rpl19*) was used as a reference. Protein extracts were obtained by homogenization of samples in a lysis buffer (50mM Tris pH 7.5, 5mM MgCl₂, 100 mM KCl, 1mM EDTA, 10% glycerol, 1mM DTT, 1%

NP40, protease and phosphatase inhibitors). Proteins were separated by SDS-PAGE and immunoblotted using antibodies against G6PC [25], phospho-AMPK α (Thr172; 2535, Cell Signaling), AMPK α (2603, Cell Signaling), phospho-ACC (3661, Cell Signaling), ACC (3676, Cell Signaling), phospho-p38 MAPK (Thr180/Tyr182, 92115, Cell Signaling), p38 MAPK (92125, Cell signaling), and AGF (sc-160959, Santa Cruz). The intensity of the bands was determined by densitometry with the system VersaDocT^M (Biorad) and analyzed using the software Quantity One[®] (Biorad).

2.8. Histological analyses. Tissues were fixed in zinc-buffered formalin and then transferred to 70% ethanol prior to processing through paraffin. Five-micrometer sections were stained with hematoxylin/eosin (H&E). Gastrocnemius muscle was frozen in isopentane cooled in liquid nitrogen. Eight-micrometer thick serial sections were obtained and processed for Succinic dehydrogenase staining as described previously [26]. **The type of fibers was discriminated by the intensity of staining. Oxidative fibers have a relatively dense, purple speckled appearance, while nonoxidative fibers have only scattered purple speckles. Oxidative type I fibers are darker than type IIa fibers while glycolytic type IIb fibers were unstained by SDH staining. The quantification of oxidative (type I+type IIa) and glycolytic fibers was performed and expressed in percent of total count fibers.**

2.9. Statistical analyses. Results are reported as means \pm SEM. The statistical analyses were performed using either a one-way ANOVA followed by Tukey's post-hoc test or a two-way ANOVA followed by Bonferroni's test. The differences were considered statistically significant at $P < 0.05$.

3. RESULTS

As a prior assessment of the effect of the hepatic deletion of G6Pase, we performed a rapid phenotyping of the L-G6pc^{-/-} mouse fed a standard carbohydrate-enriched diet. L-G6pc^{-/-} mice exhibited improved glucose tolerance during an intraperitoneal glucose challenge (Fig. S1a).

Moreover, they showed an exaggerated response to insulin injection, with dramatic drop in plasma glucose occurring at 30 min, **which required the injection of glucose at 30 min and the end of the test** (Fig. S1b). This could be the result of the incapacity of L-G6pc^{-/-} mice to mobilize liver glycogen stores [20]. However, a completely unexpected finding, which went beyond our initial question, was that L-G6pc^{-/-} mice exhibited a moderate increase in food intake compared to wild-type mice although they maintained comparable body weight gain (Fig. S1c-d). This could be due to an increase **in** energy expenditure. In keeping with this hypothesis, L-G6pc^{-/-} mice exhibited increased thermogenesis **and cold tolerance** (Fig. S1e) that was associated to an increased expression of uncoupling protein 1 (UCP1) and an increased phosphorylation of AMP-activated protein kinase α (AMPK α) in brown adipose tissue (BAT) (Fig. S1f-g). This prompted us to deepen into the phenotype linked to the deletion of **hepatic G6pc** under a HF/HS diet, extending our initial hypothesis of a resistance to diabetes to that of a possible resistance to the development of obesity that could be conferred by an increase in energy expenditure.

3.1. Resistance to diabetes and obesity in L-G6pc^{-/-} mice fed a high fat/high sucrose diet

As in mice fed a control starch diet [20], G6PC protein was undetectable in the liver of L-G6pc^{-/-} mice fed a HF/HS diet for 12 weeks (Fig. 1a). Consequently, mice showed almost complete loss of hepatic G6Pase activity (Fig. 1a). This resulted in a marked accumulation of glucose-6 phosphate (G6P) and glycogen contents in the liver of L-G6pc^{-/-} mice (Fig. 1b-c), which confirms that L-G6pc^{-/-} mice were not able to hydrolyze hepatic G6P to produce glucose. We previously showed that L-G6pc^{-/-} mice were able to maintain normal blood glucose in the fed state due to a compensatory induction of extra-hepatic glucose production driven by glucagon [20]. Similarly, glucagon levels were also twice higher in L-G6pc^{-/-} mice fed a HF/HS diet than that in wild-type mice (L-G6pc^{+/+}) (Fig. 1d). On HF/HS diet, wild-type mice exhibited impaired glucose tolerance and hyperinsulinemia (Fig. 1e). On the contrary, L-G6pc^{-/-} mice maintained glucose tolerance and basal

insulin level, and exhibited increased plasma insulin in response to glucose injection (Fig. 1e).

1 During an intraperitoneal insulin challenge, as when they were fed a control starch diet (Fig. S1b),
2
3 L-G6pc^{-/-} mice presented an exaggerated response to insulin injection, with severe hypoglycemia 30
4
5 minutes after insulin injection (Fig. 1f). We hypothesized this could be due to an enhanced
6
7 peripheral glucose uptake in L-G6pc^{-/-} mice linked to their metabolic state (Fig. S1). To better
8
9 assess insulin sensitivity, we performed a hyperinsulinemic euglycemic clamp in L-G6pc^{-/-} and
10
11 control mice fed a HF/HS diet (Table S2). EGP was totally inhibited by insulin in L-G6pc^{-/-} mice
12
13 compared to what was observed in insulin resistant wild-type mice (Table S2). These data indicate
14
15 that renal and intestinal glucose productions were sensitive to insulin inhibition in L-G6pc^{-/-} mice.
16
17 However, prior food removal being a needed condition to perform hyperinsulinemic euglycemic
18
19 clamp reliably, plasma glucose dropped rapidly from the removal of food in L-G6pc^{-/-} mice
20
21 contrarily to what happened in wild-type mice (Table S2). This might explain why we were unable
22
23 to conclude about a potential difference in peripheral glucose uptake, since glucose *per se*
24
25 influences glucose uptake independently of plasma insulin [27]. On the other hand, basal 2-
26
27 deoxyglucose uptake was significantly enhanced not only in the BAT but also in most insulin-
28
29 sensitive tissues, such as the long digital extensor (LDE) muscle and the subcutaneous and gonadal
30
31 WAT in L-G6pc^{-/-} mice (Fig. 1g). This was in agreement with our hypothesis of enhanced
32
33 peripheral glucose metabolism in these mice. Finally, L-G6pc^{-/-} mice failed to develop fasting
34
35 hyperglycemia, contrarily to wild-type mice whose blood glucose exceeded 150 mg/dL after 16
36
37 hours of fasting (Fig. 1h). These results indicate that L-G6pc^{-/-} mice resisted the development of
38
39 diabetes, not only due to the absence of HGP, but also due to events taking place in peripheral
40
41 tissues.
42
43
44
45
46
47
48
49
50

51 As hypothesized from the results of Fig. S1, L-G6pc^{-/-} mice resisted the development of diet-
52
53 induced obesity (Fig. 2a-b). Indeed, L-G6pc^{-/-} mice failed to gain weight on a HF/HS diet, contrarily
54
55 to wild-type mice, despite identical food intake (Fig. 2c). DEXA analysis revealed that body fat mass
56
57
58
59
60
61
62
63
64
65

1 represented only 25% of total body mass in L-G6pc^{-/-} mice compared to 45% in control mice (Fig.
2 2d), without modification of lean mass (not shown), and individual fat pads weighed significantly
3 less in L-G6pc^{-/-} mice (Fig. 2e). Consistent with reduced fat mass, plasma leptin levels were
4 markedy reduced in L-G6pc^{-/-} mice compared to wild-type mice, whilst adiponectin levels were not
5 altered (Fig. 2f). Concomitantly to the development of obesity, HF/HS diet is known to induce
6 hepatic steatosis as observed in C57Bl/6J control mice (Fig. S2). We then evaluated triglyceride
7 accumulation in livers of L-G6pc^{-/-} compared to control mice fed a HF/HS diet. Histological
8 analyses showed differential zonation of triglycerides in livers of L-G6pc^{-/-} and control mice.
9 Control mice accumulated lipid droplets in the perivenous region, the preferential site for glycolysis
10 and lipogenesis [28], while L-G6pc^{-/-} mice accumulated fat in the periportal region, dedicated to
11 gluconeogenesis, which corresponds to G6Pase histological localization [25]. In accordance to what
12 we previously observed after 9 months of HF/HS diet [29], L-G6pc^{-/-} mice showed reduced hepatic
13 triglyceride accumulation compared to control mice (Fig. S2b). No inflammation was observed on
14 histological liver slides of L-G6pc^{-/-} livers. Moreover, L-G6pc^{-/-} mice showed reduced liver
15 inflammation reflected by lower expression of TNF α (Fig. S2c). In addition, picrosirius red staining
16 showed no fibrosis (Fig. S2d). All together, these data suggest an amelioration of hepatic steatosis
17 in L-G6pc^{-/-} mice on HF/HS diet, despite severe lipogenic flux [21]. Thus, the specific suppression
18 of HGP prevented the onset of T2D as well as diet-induced obesity.
19
20
21
22
23
24
25
26
27
28
29
30
31
32
33
34
35
36
37
38
39
40
41
42
43
44

45 **3.2. The absence of hepatic glucose production stimulates energy expenditure and adaptive** 46 **thermogenesis** 47

48 We then questioned the mechanisms underlying obesity resistance in L-G6pc^{-/-} mice. Basal physical
49 activity was similar for L-G6pc^{-/-} and L-G6pc^{+/+} mice (Fig. 3a). Indirect calorimetric measurements
50 revealed increased basal metabolic rate in L-G6pc^{-/-} mice and increased whole-body oxygen
51 consumption (Fig. 3b-c). This was associated with the induction of thermogenesis, manifested by
52
53
54
55
56
57
58
59
60
61
62
63
64
65

increased rectal temperature in L-G6pc^{-/-} mice (Fig. 3d). Interestingly, free fatty acids (FFA), which are potent inducers of uncoupling protein (UCP) transcription [30], were two-fold higher in L-G6pc^{-/-} mice (Fig. 3e). At the molecular level, the skeletal muscles of L-G6pc^{-/-} mice showed remarkable overexpression of proliferator-activated receptors (PPAR α and PPAR δ) and their coactivator PGC1 α , major regulators of energy metabolism [30,31]. This was associated with up-regulation of UCP2 and UCP3 uncoupling proteins, of the genes encoding elements of the respiratory chain (*Cox4* and *Cytsc*), and of a number of target genes involved in fatty acid uptake and oxidation (*Cd36*, *Lpl*, *Acox1*, and *Cpt1b*) (Fig. 3f). These data were correlated with an increase in the rate of oxygen consumption during the ADP-stimulated state (state 3) in mitochondria isolated from L-G6pc^{-/-} mice skeletal muscle compared to wild-type mice. In accordance with the induced expression of *Cox4* gene (Fig. 3f), the respiration rate associated with cytochrome c oxidase activity was also higher in the mitochondria isolated from L-G6pc^{-/-} mice compared to wild-type mice (Fig. 3g). These data confirm increased mitochondrial oxidative capacities in the muscles of L-G6pc^{-/-} mice. Concomitantly, AMP-activated protein kinase (AMPK) and p38 mitogen-activated protein kinase (P38MAPK), regulators of both energy expenditure and mitochondrial biogenesis [32,33], were hyper-phosphorylated in the muscles of L-G6pc^{-/-} mice compared to those of control mice (2.8-fold induction for P-AMPK, p<0.001; 1.5-fold induction for P38MAPK, p<0.05 in L-G6pc^{-/-} mice compared to control mice). The activation of AMPK was accompanied by an increased phosphorylation of ACC (2-fold induction, p<0.01), a mechanism known to decrease its activity and stimulate fatty acid oxidation (Fig. 3h). PGC1 α , PPAR δ and AMPK are all critical regulators of the muscle fiber type switch [33–35], mediating the transformation of glycolytic type IIb muscle fibers to oxidative type IIa or type I fibers. Accordingly, *in situ* succinate dehydrogenase staining revealed remodeling of the gastrocnemius muscle in L-G6pc^{-/-} mice, with an increase in the proportion of oxidative fibers compared to control mice (Fig. 3i) and an increase of the expression of slow myosin heavy chain isoform (MHC1) (8-fold induction, p<0.05 in L-G6pc^{-/-} mice compared

1 to control mice), which is specifically expressed in type I fibers (Fig. 3j). Interestingly, the
2 metabolic modifications observed in the L-G6pc^{-/-} muscles mimic muscle adaptations observed
3 following a regular endurance exercise. Unfortunately, L-G6pc^{-/-} mice could not run as long as
4 wild-type mice since they developed a dramatic hypoglycemia during activity on treadmill (Table
5 S3). However, we could note that L-G6pc^{-/-} mice showed a higher acceleration than wild-type mice
6 during an acute high intensity exercise (physical activity wheels) (Table S3). Thus, these data
7 suggest a metabolic transformation of L-G6pc^{-/-} skeletal muscle into an oxidative phenotype.
8 Concomitantly, thermogenesis was also induced in both BAT and WAT of L-G6pc^{-/-} mice. This
9 was shown by the overexpression of *Ucp1*, associated to the activation of the AMPK pathway (2.7-
10 fold induction for P-AMPK α in BAT, p<0.001 and 4.7-fold induction in WAT of L-G6pc^{-/-} mice,
11 p<0.05 compared to control mice) (Fig. 4a-b). Histological analysis revealed a different
12 morphology of WAT and BAT in L-G6pc^{-/-} mice, with less accumulation of fat droplets in BAT
13 (Fig. 4a) and smaller adipocytes in subcutaneous WAT (Fig. 4b).
14 These data indicate that the absence of HGP triggered a remodeling program in the muscles, WAT
15 and BAT in L-G6pc^{-/-} mice, leading to an increased oxidative capacity, energy metabolism and
16 thermogenesis. It is noteworthy to mention here that a number of parameters altered in L-G6pc^{-/-}
17 mice under HF/HS were also comparably altered under standard starch feeding, encompassing the
18 mRNA levels of *Ppar*, *Cyt1b*, *Cytcs*, *Cox4*, *Ucp2*, *Ucp3* and the phosphorylation state of AMPK in
19 skeletal muscle (data not shown, see also Fig. S1).
20
21
22
23
24
25
26
27
28
29
30
31
32
33
34
35
36
37
38
39
40
41
42
43
44

45 **3.3. The suppression of hepatic glucose production induces the expression of hepatic** 46 **metabolic regulators of energy homeostasis** 47

48 We then questioned the mechanisms by which the specific inactivation of G6Pase in the liver could
49 mediate its effects on glucose and energy metabolism in peripheral tissues. First, we assessed
50 whether the effects of hepatic G6PC deletion were mediated by a neural signal ascending from the
51
52
53
54
55
56
57
58
59
60
61
62
63
64
65

liver to the brain through the afferent vagus [36,37], or by a portal-brain neural communication initiated by intestinal gluconeogenesis [17,19,38]. We applied an afferent-specific neurotoxin, capsaicin, to the hepatic branch of the vagus nerve and the portal area of L-G6pc^{-/-} and control mice. The denervation of hepato-portal afferents did not modify insulin sensitivity or glucose tolerance of L-G6pc^{-/-} (Fig. S3), which excludes the possibility of a neural signal from the liver or the portal vein linking hepatic G6Pase inactivation with enhanced glucose metabolism in L-G6pc^{-/-} mice. Second, we assessed the expression of a number of liver secreted factors, also named hepatokines, which are known to affect peripheral glucose metabolism, insulin sensitivity and energy expenditure [39–43]. L-G6pc^{-/-} mice showed no change in expression of the hepatic growth factor (HGF), selenoprotein P (SeP), fetuin-A, and a slightly decreased expression of insulin-like growth factor-1 (IGF1), adropin (Enho for Energy homeostasis associated protein) and angiopoietin-like growth factor 3 (Angptl3) (Fig. 5a). On the other hand, there was dramatic overexpression of fibroblast growth factor 21 (FGF21) mRNA in the livers of L-G6pc^{-/-} mice (Fig. 5a), which was associated with a marked increase in the level of circulating FGF21 plasma (Fig. 5b). FGF21 has recently emerged as a major regulator of glucose and energy metabolism, with WAT as a major site for its anti-obesity action [44–46] In the liver, FGF21 induces gluconeogenesis, fatty acid oxidation, triglyceride clearance, and ketogenesis. To characterize the hepatic effects of FGF21 was out of the scope of the present study. Moreover, they were highlighted in a number of recent papers [44,47–50]. In the light of the results above, we estimated the role of FGF21 overexpression in the peripheral metabolic phenotype of L-G6pc^{-/-} mice. For that, we abolished the expression of FGF21 by crossing B6.FGF21^{-/-} mice [22] with B6.G6pc^{lox/lox}.SACre^{ERT2} mice. After tamoxifen treatment, L-G6pc^{-/-}.FGF21^{-/-} (DKO) mice exhibited a metabolic phenotype comparable to that of L-G6pc^{-/-} mice and also resisted diabetes and obesity (Fig.5 d-f). However, these mice had less subcutaneous WAT than wild-type mice (Fig. 5g), but without modification of leptin and adiponectin levels (data not shown). At the molecular level, the UCP1 protein level of L-G6pc^{-/-}.FGF21^{-/-} mice was restored to that of control

1 mice and much lower than that of L-G6pc^{-/-} mice (Fig. 5h). A comparable result was observed at
2 mRNA level (Fig. S4a). However, this was not sufficient to inverse the whole body metabolic
3 benefits linked to hepatic G6Pase deficiency. Thus, these data suggest a major role of FGF21 on the
4 enhanced glucose metabolism of WAT in L-G6pc^{-/-} mice. However, the overexpression of FGF21
5
6 *per se* could not explain the enhanced whole body glucose and energy metabolism due to the
7
8 absence of liver G6Pase. Interestingly, L-G6pc^{-/-} mice exhibited marked overexpression of
9
10 angiopoietin-like growth factor-4 (Angptl4 or FIAF for Fasting-Induced Adipose tissue Factor) and
11
12 angiopoietin-like growth factor-6 (Angptl6 or AGF for Angiopoietin-related Growth Factor) mRNA
13
14 in the liver (Fig. 5a), that was associated with an increase of AGF plasma level (Fig. 5c). FIAF has
15
16 been suggested to exert beneficial effects on glucose control whereas this issue remains
17
18 controversial [39]. On the other hand, AGF is a major activator of peripheral energy expenditure,
19
20 through activation of adaptive thermogenesis in skeletal muscle and BAT [51]. Thus, AGF might
21
22 account for the changes observed in the skeletal muscles and BAT of L-G6pc^{-/-} mice. Interestingly,
23
24 the expression of these hepatokines was not modified in L-G6pc^{-/-}.FGF21^{-/-} mice compared to that
25
26 in L-G6pc^{-/-} mice (Fig. S4c). It is interesting to note that FGF21 and AGF plasmatic concentrations
27
28 were increased in L-G6pc^{-/-} mice fed a control starch diet (data not shown).
29
30
31
32
33
34
35
36

37 On a mechanistic viewpoint, the metabolic state of the liver deriving from the deletion of *G6pc*
38
39 (increased G6P level and steatosis) might account for the increased expression of FGF21 and
40
41 ANGPTLs. Indeed, the expression of the latter is increased in fatty livers [39,42]. Moreover, the
42
43 Carbohydrate Response Element Binding Protein (ChREBP) activates the transcription of the
44
45 FGF21 gene [52]. The activation state of ChREBP was highlighted here *via* the increased gene
46
47 expression of *Pklr*, *Acaca* and *Fasn* (Fig. S4d), which are canonical targets of this transcription
48
49 factor [53]. This was in keeping with the increased liver G6P content (Fig. 1b), the latter being the
50
51 major activator of the lipogenic transcription factor [54]. In addition, the expression of ChREBP
52
53 protein (isoforms A and B [55]) was induced in both L-G6pc^{-/-} and L-G6pc^{-/-}.FGF21^{-/-} mice,
54
55
56
57
58
59
60
61
62
63
64
65

compared to control mice (Fig. 5i).

3.4. The suppression of hepatic glucose production corrects **insulin resistance** and stabilizes **obesity in previously obese and diabetic mice**

Since the absence of HGP prevented the onset of obesity and preserved leanness in L-G6pc^{-/-} mice, this could account at least in part for their improved glucose control. Thus, we wondered whether the specific suppression of HGP would be sufficient to improve metabolic control in previously obese and **insulin-resistant** mice. Floxed *G6pc* (B6.SA^{CreERT2}.G6pc^{lox/lox}) mice and C57Bl/6J mice were first fed a HF/HS diet for 16 weeks prior to inducing *G6pc* deletion. Floxed *G6pc* mice became obese **and insulin-resistant and showed fasting hyperglycemia** as observed with control mice (Fig. 6a-c). Interestingly, the overnight fasting glucose and insulin levels were normalized after only 10 days of treatment by tamoxifen that deleted hepatic *G6pc* (Fig. 6a-b). Concomitantly, glucose tolerance was markedly improved in obese diabetic L-G6pc^{-/-} mice (od.L-G6pc^{-/-}), compared to glucose tolerance before liver *G6pc* deletion (Fig. 6c) and compared to control mice (Fig. 1e). Hypersensitivity to insulin was also seen 3 weeks after the HGP blockade (Fig. 6d). It is noteworthy that these improvements in glucose metabolism took place early, in mice that were still obese, before **any** difference in body weight was observed **compared to** control mice (Fig. 6e), which indicates that they were not dependent on a change in body weight or on leanness. The inactivation of **hepatic** G6Pase did not promote weight loss in od.L-G6pc^{-/-} mice. However, it induced the stabilization of their body weight and prevented further weight gain on the HF/HS diet (Fig. 6e), without modification of food intake (data not shown). In addition, od.L-G6pc^{-/-} mice exhibited diminished subcutaneous WAT and a decrease in leptin level compared to wild-type mice (Fig. 6f-g). Moreover, they showed a general induction of the thermogenic and remodeling program in skeletal muscle, BAT and WAT (Fig. 6h-j). A key observation was that the loss of **hepatic**

1 G6Pase in od.L-G6pc^{-/-} mice was associated with the induction of both hepatic FGF21 and AGF
2 expression and protein circulating levels (Fig. 6k).
3
4
5

6 **4. DISCUSSION**

7
8 According to the current dogma, the increase in EGP would be a crucial event during the
9 development of IR, which could play a key role in the appearance of fasting hyperglycemia
10 associated to T2D [6,7,10]. In line with this rationale, we show here that the absence of HGP, a
11 major component of EGP, efficiently protected mice from the development of hyperglycemia on
12 HF/HS diet. What was more intriguing was that the benefits of HGP suppression went beyond the
13 prevention of fasting hyperglycemia to modulate three major players in the pathogenesis of T2D:
14 obesity, peripheral glucose handling, and **hepatic** metabolism. Moreover, the specific suppression of
15 HGP rapidly normalized glucose **control** and insulin action in previously obese and diabetic mice.
16
17

18 The controlling role of HGP on peripheral glucose and energy metabolism is the major
19 breakthrough of this study. HGP suppression led to **the maintenance of** leanness and enhancement
20 of glucose handling *via* the induction of adaptive thermogenesis in WAT, BAT and skeletal muscle
21 in L-G6pc^{-/-} mice. The activation of thermogenesis is considered to be an attractive approach for
22 counteracting obesity and related glucose intolerance [30,31]. In particular, the loss of **hepatic**
23 G6Pase led to a profound transformation of skeletal muscle into an oxidative phenotype that mimics
24 the effects of physical exercise and endurance training on skeletal muscle metabolism [26,56–58].
25 In addition to its anti-obesity effect, the increased muscular oxidative capacity could account for
26 protection against IR through the attenuation of triglyceride accumulation [59]. Moreover, the
27 activation of P38MAPK and AMPK in skeletal muscles of L-G6pc^{-/-} mice probably mediates
28 increased basal- and insulin-stimulated glucose uptake in a contraction-like manner [60,61]. These
29 findings place HGP in a central position in the regulation of whole-body glucose and energy
30 metabolism. It is noteworthy that the first-line oral glucose-lowering drug recommended in the
31
32
33
34
35
36
37
38
39
40
41
42
43
44
45
46
47
48
49
50
51
52
53
54
55
56
57
58
59
60
61
62
63
64
65

guidelines of the American Diabetes Association and European Association for the Study of

Diabetes is metformin. The main action of metformin is to decrease hepatic glucose output, **through** the suppression of the metabolic flux through G6Pase, promoting increased G6P content [62].

Reports have previously shown that metformin activates AMPK and increases glucose uptake in skeletal muscle of treated diabetic patients [63], although metformin is known to accumulate preferentially in the liver and intestine [64]. Thus, our results provide an alternative explanation for the activation of muscle AMPK by metformin *in vivo*. **It is interesting to mention that, independently of their possible adverse effects, anti-diabetic strategies based on the use of hepatic G6Pase inhibitors promote hepatic changes comparable to those in L-G6pc^{-/-} mice or in metformin-treated rats and revealed very efficient to combat the disease [65].**

Suppressing hepatic G6Pase activity as a cure for diabetes is a long proposed idea. This would be difficult to achieve without risking severe hypoglycemic episodes and perhaps the adverse hepatic effects seen in G6Pase deficiency, such as severe hepatic steatosis or development of lactic acidosis. However, deriving the metabolic flux from gluconeogenesis flow into lipogenesis (**like it** occurs in L-G6pc^{-/-} mice) has been compellingly shown to improve **glucose control** [66,67]. It is noteworthy that a partial suppression of hepatic G6Pase activity associated to increased G6P content was achievable through the induction of intestinal gluconeogenesis in favorable metabolic situations **such** as gastric bypass or fiber feeding [19,38] or metformin treatment (see above). Moreover, this study provides a new paradigm highlighting the beneficial consequences of a better HGP control. Indeed, the inhibition of HGP is shown here to result in increased secretion of at least two key hepatic **regulators of peripheral metabolism**: FGF21 and AGF, as a likely consequence of the G6P-mediated activation of ChREBP. FGF21 is a potent regulator of whole-body glucose and energy metabolism [46,48,68]. The stimulation of peripheral glucose uptake by FGF21 is restricted to WAT, where it induces insulin-independent glucose uptake and potentiates insulin-stimulated glucose uptake [46,69]. FGF21 also increases energy expenditure in WAT, through activation of the

1 AMPK/PGC1a/Sirt1 axis and induction of a BAT-like phenotype, including induced expression of
2 UCP1 as a key endpoint. It is noteworthy that UCP expression was restored to normal in L-G6pc^{-/-}
3 .FGF21^{-/-} mice, which firmly indicates a causal role for FGF21 in the WAT phenotype of L-G6pc^{-/-}
4 mice. Similar experiments to assess the causal role of AGF in the muscle phenotype were not
5 undergone. Indeed, the **homozygous** AGF-KO mice are not viable [51] and the **heterozygous** KO
6 would hardly achieve a plasmatic suppression of the factor sufficient to restore to normal the
7 muscle gene expression program, especially under conditions of increased AGF expression in the
8 liver. However, AGF is a potent modulator of adaptive thermogenesis in skeletal muscle and BAT,
9 through the activation of PPARs and PGCs, P38 MAPK, and the expression of uncoupling proteins,
10 which leads to increased energy expenditure and associated enhancement of insulin sensitivity
11 [39,51]. Thus, the concomitant induction of both hepatic regulators FGF21 and AGF in L.G6pc^{-/-}
12 mice could clearly account for the benefits observed on whole-body metabolism. **It is noteworthy**
13 **that the first trials using FGF21 analogs alone or in combination with other hormones (e.g. leptin or**
14 **glucagon-like peptide 1) revealed promising in the treatment of metabolic diseases [70–73].**
15 **Moreover, the interest to combine different hormones in chimeric protein has been recently**
16 **highlighted [74]. Thus, our results suggest that the association of FGF21 and AGF, combined or not**
17 **with an approach targeting hepatic glucose production, could appear attractive strategies for future**
18 **treatments of obesity and type 2 diabetes.**

49 5. CONCLUSION

50 On a conceptual viewpoint, in addition to the metabolic benefits linked to the increased glucose
51 production from the intestine [19,38], the data reported here emphasize that HGP should no longer
52 be equaled to EGP. **Moreover, we** point out that the control of HGP *per se* could be a crucial
53 objective in the management of metabolic diseases taken as a whole. This means not only to prevent
54
55
56
57
58
59
60
61
62
63
64
65

1 or treat increased fasting hyperglycemia and related glucotoxicity of diabetes, but also to initiate an
2 integrated hormonal and/or metabolic crosstalk modulating the different components involved in
3 the onset of the illness, including obesity and peripheral IR. These data open novel perspectives in
4 the understanding of metabolic diseases in general and diabetes in particular.
5
6
7
8
9
10
11
12

13 **ACKNOWLEDGMENTS**

14
15 We would like to thank Dr David Mangelsdorf and Dr Steven Kliewer (The University of Texas
16 Southwestern Medical Center, Dallas, US) for generously providing B6.Fgf21^{-/-} mice, Dr. Fabien
17 Delaere for capsaicin treatment, Prof Claude Duchamp (UMR5023 CNRS, University Lyon1) for
18 helpful discussion about mitochondrial respiration in muscles, the members of the Aniphys platform
19 (Faculté de médecine Lyon-Est, Lyon), Angèle Chamousset and Jean-Michel Vicat for animal care
20 (*Animalerie Lyon Est Conventiionnelle et SPF*, Université Lyon 1 Laennec, SFR Santé Lyon-Est,
21 Lyon), the members of the Anipath Platform (Université Lyon 1 Laennec) and Norbert Laroche for
22 Dexa analyses (Université Jean Monnet, St-Etienne). This work was supported by research grants
23 from the “Fondation pour la recherche médicale” (project n°DRM20121220448) and the “Société
24 francophone du diabète” (project IT 08290 Alfediam/BMS2008 and SFD/Takeda 2010). Aya
25 Abdul-Wahed received a grant from the Ministry of Higher Education of the Syrian Arab Republic
26 and from the “Fondation pour la recherche médicale”.
27
28
29
30
31
32
33
34
35
36
37
38
39
40
41
42
43
44
45
46

47 **CONFLICT OF INTEREST**

48
49 The authors declare that they have no conflict of interest to disclose in relation to this work.
50
51
52
53
54
55
56
57
58
59
60
61
62
63
64
65

REFERENCES

- 1 [1] L. Chen, D.J. Magliano, P.Z. Zimmet, The worldwide epidemiology of type 2 diabetes
2 mellitus--present and future perspectives, *Nat. Rev. Endocrinol.* 8 (2012) 228–236.
3
4
5
6 [2] R.A. DeFronzo, Pathogenesis of type 2 diabetes mellitus, *Med. Clin. North Am.* 88 (2004)
7 787–835, ix.
8
9
10 [3] D.K. Granner, R.M. O'Brien, Molecular physiology and genetics of NIDDM. Importance of
11 metabolic staging, *Diabetes Care.* 15 (1992) 369–395.
12
13
14
15 [4] C. Weyer, C. Bogardus, D.M. Mott, R.E. Pratley, The natural history of insulin secretory
16 dysfunction and insulin resistance in the pathogenesis of type 2 diabetes mellitus, *J. Clin.*
17 *Invest.* 104 (1999) 787–794.
18
19
20
21
22 [5] D. Lauro, Y. Kido, A.L. Castle, M.J. Zarnowski, H. Hayashi, Y. Ebina, et al., Impaired
23 glucose tolerance in mice with a targeted impairment of insulin action in muscle and adipose
24 tissue, *Nat. Genet.* 20 (1998) 294–298.
25
26
27
28
29 [6] J.N. Clore, J. Stillman, H. Sugerma, Glucose-6-phosphatase flux in vitro is increased in type
30 2 diabetes, *Diabetes.* 49 (2000) 969–974.
31
32
33
34 [7] A. Consoli, N. Nurjhan, F. Capani, J. Gerich, Predominant role of gluconeogenesis in
35 increased hepatic glucose production in NIDDM, *Diabetes.* 38 (1989) 550–557.
36
37
38
39 [8] P.D. Home, G. Pacini, Hepatic dysfunction and insulin insensitivity in type 2 diabetes
40 mellitus: a critical target for insulin-sensitizing agents, *Diabetes Obes. Metab.* 10 (2008) 699–
41 718.
42
43
44
45 [9] I. Magnusson, D.L. Rothman, L.D. Katz, R.G. Shulman, G.I. Shulman, Increased rate of
46 gluconeogenesis in type II diabetes mellitus. A ¹³C nuclear magnetic resonance study, *J. Clin.*
47 *Invest.* 90 (1992) 1323–1327.
48
49
50
51
52 [10] R.A. Rizza, Pathogenesis of fasting and postprandial hyperglycemia in type 2 diabetes:
53 implications for therapy, *Diabetes.* 59 (2010) 2697–2707.
54
55
56
57
58
59
60
61
62
63
64
65

- 1
2
3
4
5
6
7
8
9
10
11
12
13
14
15
16
17
18
19
20
21
22
23
24
25
26
27
28
29
30
31
32
33
34
35
36
37
38
39
40
41
42
43
44
45
46
47
48
49
50
51
52
53
54
55
56
57
58
59
60
61
62
63
64
65
- [11] M. Roden, K.F. Petersen, G.I. Shulman, Nuclear magnetic resonance studies of hepatic glucose metabolism in humans, *Recent Prog. Horm. Res.* 56 (2001) 219–237.
- [12] J.Y. Altarejos, M. Montminy, CREB and the CRTC co-activators: sensors for hormonal and metabolic signals, *Nat. Rev. Mol. Cell Biol.* 12 (2011) 141–151.
- [13] S. Del Prato, P. Marchetti, Beta- and alpha-cell dysfunction in type 2 diabetes, *Horm. Metab. Res.* 36 (2004) 775–781.
- [14] G. Mithieux, F. Rajas, A. Gautier-Stein, A novel role for glucose 6-phosphatase in the small intestine in the control of glucose homeostasis, *J. Biol. Chem.* 279 (2004) 44231–44234.
- [15] F. Delaere, C. Magnan, G. Mithieux, Hypothalamic integration of portal glucose signals and control of food intake and insulin sensitivity, *Diabetes Metab.* 36 (2010) 257–262.
- [16] G. Mithieux, Nutrient control of hunger by extrinsic gastrointestinal neurons, *Trends Endocrinol. Metab. TEM.* 24 (2013) 378–384.
- [17] C. Duraffourd, F. De Vadder, D. Goncalves, F. Delaere, A. Penhoat, B. Brusset, et al., Mu-opioid receptors and dietary protein stimulate a gut-brain neural circuitry limiting food intake, *Cell.* 150 (2012) 377–388.
- [18] B. Pillot, M. Soty, A. Gautier-Stein, C. Zitoun, G. Mithieux, Protein feeding promotes redistribution of endogenous glucose production to the kidney and potentiates its suppression by insulin, *Endocrinology.* 150 (2009) 616–624.
- [19] F. De Vadder, P. Kovatcheva-Datchary, D. Goncalves, J. Vinera, C. Zitoun, A. Duchamp, et al., Microbiota-generated metabolites promote metabolic benefits via gut-brain neural circuits, *Cell.* 156 (2014) 84–96.
- [20] E. Mutel, A. Gautier-Stein, A. Abdul-Wahed, M. Amigó-Correig, C. Zitoun, A. Stefanutti, et al., Control of blood glucose in the absence of hepatic glucose production during prolonged fasting in mice: induction of renal and intestinal gluconeogenesis by glucagon, *Diabetes.* 60 (2011) 3121–3131.

- 1
2
3
4
5
6
7
8
9
10
11
12
13
14
15
16
17
18
19
20
21
22
23
24
25
26
27
28
29
30
31
32
33
34
35
36
37
38
39
40
41
42
43
44
45
46
47
48
49
50
51
52
53
54
55
56
57
58
59
60
61
62
63
64
65
- [21] E. Mutel, A. Abdul-Wahed, N. Ramamonjisoa, A. Stefanutti, I. Houberton, S. Cavassila, et al., Targeted deletion of liver glucose-6 phosphatase mimics glycogen storage disease type 1a including development of multiple adenomas, *J. Hepatol.* 54 (2011) 529–537.
- [22] M.J. Potthoff, T. Inagaki, S. Satapati, X. Ding, T. He, R. Goetz, et al., FGF21 induces PGC-1alpha and regulates carbohydrate and fatty acid metabolism during the adaptive starvation response, *Proc. Natl. Acad. Sci. U. S. A.* 106 (2009) 10853–10858.
- [23] T.J. Wetter, A.C. Gazdag, D.J. Dean, G.D. Cartee, Effect of calorie restriction on in vivo glucose metabolism by individual tissues in rats, *Am. J. Physiol.* 276 (1999) E728–738.
- [24] G. Pfeleiderer, Glycogen: determination with amyloglucosidase, in: *Methods Enzym. Anal.*, 2nd ed., Bergmeyer HU, Deerfield Beach, FL, US, 1974: pp. 59–62.
- [25] F. Rajas, H. Jourdan-Pineau, A. Stefanutti, E.A. Mrad, P.B. Iynedjian, G. Mithieux, Immunocytochemical localization of glucose 6-phosphatase and cytosolic phosphoenolpyruvate carboxykinase in gluconeogenic tissues reveals unsuspected metabolic zonation, *Histochem. Cell Biol.* 127 (2007) 555–565.
- [26] S. Luquet, J. Lopez-Soriano, D. Holst, A. Fredenrich, J. Melki, M. Rassoulzadegan, et al., Peroxisome proliferator-activated receptor delta controls muscle development and oxidative capability, *FASEB J. Off. Publ. Fed. Am. Soc. Exp. Biol.* 17 (2003) 2299–2301.
- [27] G. Mithieux, A. Gautier-Stein, F. Rajas, C. Zitoun, Contribution of intestine and kidney to glucose fluxes in different nutritional states in rat, *Comp. Biochem. Physiol. B Biochem. Mol. Biol.* 143 (2006) 195–200.
- [28] C. Postic, J. Girard, Contribution of de novo fatty acid synthesis to hepatic steatosis and insulin resistance: lessons from genetically engineered mice, *J. Clin. Invest.* 118 (2008) 829–838.

- 1 hepatic lipid quantification using MRS at 7 Tesla in a mouse model of glycogen storage
2 disease type 1a, *J. Lipid Res.* 54 (2013) 2010–2022.
- 3
4
5
6 [30] B.B. Lowell, B.M. Spiegelman, Towards a molecular understanding of adaptive
7 thermogenesis, *Nature*. 404 (2000) 652–660.
- 8
9
10 [31] R.M. Evans, G.D. Barish, Y.-X. Wang, PPARs and the complex journey to obesity, *Nat. Med.*
11
12 10 (2004) 355–361.
- 13
14
15 [32] A.R. Pogozielski, T. Geng, P. Li, X. Yin, V.A. Lira, M. Zhang, et al., p38gamma mitogen-
16 activated protein kinase is a key regulator in skeletal muscle metabolic adaptation in mice,
17
18 *PloS One*. 4 (2009) e7934.
- 19
20
21
22 [33] B. Viollet, L. Lantier, J. Devin-Leclerc, S. Hebrard, C. Amouyal, R. Mounier, et al., Targeting
23 the AMPK pathway for the treatment of Type 2 diabetes, *Front. Biosci. Landmark Ed.* 14
24
25 (2009) 3380–3400.
- 26
27
28
29 [34] E. Ehrenborg, A. Krook, Regulation of skeletal muscle physiology and metabolism by
30 peroxisome proliferator-activated receptor delta, *Pharmacol. Rev.* 61 (2009) 373–393.
- 31
32
33 [35] J. Olesen, K. Küllerich, H. Pilegaard, PGC-1alpha-mediated adaptations in skeletal muscle,
34
35 *Pflüg. Arch. Eur. J. Physiol.* 460 (2010) 153–162.
- 36
37
38 [36] J. Imai, H. Katagiri, T. Yamada, Y. Ishigaki, T. Suzuki, H. Kudo, et al., Regulation of
39 pancreatic beta cell mass by neuronal signals from the liver, *Science*. 322 (2008) 1250–1254.
- 40
41
42 [37] K. Uno, H. Katagiri, T. Yamada, Y. Ishigaki, T. Ogihara, J. Imai, et al., Neuronal pathway
43 from the liver modulates energy expenditure and systemic insulin sensitivity, *Science*. 312
44
45 (2006) 1656–1659.
- 46
47
48 [38] S. Troy, M. Soty, L. Ribeiro, L. Laval, S. Migrenne, X. Fioramonti, et al., Intestinal
49 gluconeogenesis is a key factor for early metabolic changes after gastric bypass but not after
50 gastric lap-band in mice, *Cell Metab.* 8 (2008) 201–211.
- 51
52
53
54
55
56
57
58
59
60
61
62
63
64
65

- 1
2
3
4
5
6
7
8
9
10
11
12
13
14
15
16
17
18
19
20
21
22
23
24
25
26
27
28
29
30
31
32
33
34
35
36
37
38
39
40
41
42
43
44
45
46
47
48
49
50
51
52
53
54
55
56
57
58
59
60
61
62
63
64
65
- [39] Y. Oike, M. Akao, Y. Kubota, T. Suda, Angiopoietin-like proteins: potential new targets for metabolic syndrome therapy, *Trends Mol. Med.* 11 (2005) 473–479.
- [40] K.G. Kumar, J.L. Trevaskis, D.D. Lam, G.M. Sutton, R.A. Koza, V.N. Chouljenko, et al., Identification of adropin as a secreted factor linking dietary macronutrient intake with energy homeostasis and lipid metabolism, *Cell Metab.* 8 (2008) 468–481.
- [41] G. Perdomo, M.A. Martinez-Brocca, B.A. Bhatt, N.F. Brown, R.M. O’Doherty, A. Garcia-Ocaña, Hepatocyte growth factor is a novel stimulator of glucose uptake and metabolism in skeletal muscle cells, *J. Biol. Chem.* 283 (2008) 13700–13706.
- [42] N. Stefan, H.-U. Häring, Circulating fetuin-A and free fatty acids interact to predict insulin resistance in humans, *Nat. Med.* 19 (2013) 394–395.
- [43] K.M. Habegger, K. Stemmer, C. Cheng, T.D. Muller, K.M. Heppner, N. Ottaway, et al., Fibroblast Growth Factor 21 Mediates Specific Glucagon Actions, *Diabetes.* 62 (2013) 1453–1463.
- [44] M.K. Badman, P. Pissios, A.R. Kennedy, G. Koukos, J.S. Flier, E. Maratos-Flier, Hepatic fibroblast growth factor 21 is regulated by PPARalpha and is a key mediator of hepatic lipid metabolism in ketotic states, *Cell Metab.* 5 (2007) 426–437.
- [45] A. Kharitonkov, P. Larsen, FGF21 reloaded: challenges of a rapidly growing field, *Trends Endocrinol. Metab. TEM.* 22 (2011) 81–86.
- [46] A. Kharitonkov, T.L. Shiyanova, A. Koester, A.M. Ford, R. Micanovic, E.J. Galbreath, et al., FGF-21 as a novel metabolic regulator, *J. Clin. Invest.* 115 (2005) 1627–1635.
- [47] E.D. Berglund, C.Y. Li, H.A. Bina, S.E. Lynes, M.D. Michael, A.B. Shanafelt, et al., Fibroblast growth factor 21 controls glycemia via regulation of hepatic glucose flux and insulin sensitivity, *Endocrinology.* 150 (2009) 4084–4093.
- [48] T. Coskun, H.A. Bina, M.A. Schneider, J.D. Dunbar, C.C. Hu, Y. Chen, et al., Fibroblast growth factor 21 corrects obesity in mice, *Endocrinology.* 149 (2008) 6018–6027.

- [49] Y. Li, K. Wong, A. Giles, J. Jiang, J.W. Lee, A.C. Adams, et al., Hepatic SIRT1 Attenuates Hepatic Steatosis and Controls Energy Balance in Mice by Inducing Fibroblast Growth Factor 21, *Gastroenterology*. 146 (2014) 539–549.
- [50] J. Xu, D.J. Lloyd, C. Hale, S. Stanislaus, M. Chen, G. Sivits, et al., Fibroblast growth factor 21 reverses hepatic steatosis, increases energy expenditure, and improves insulin sensitivity in diet-induced obese mice, *Diabetes*. 58 (2009) 250–259.
- [51] Y. Oike, M. Akao, K. Yasunaga, T. Yamauchi, T. Morisada, Y. Ito, et al., Angiopoietin-related growth factor antagonizes obesity and insulin resistance, *Nat. Med.* 11 (2005) 400–408.
- [52] T. Uebanso, Y. Taketani, H. Yamamoto, K. Amo, H. Ominami, H. Arai, et al., Paradoxical regulation of human FGF21 by both fasting and feeding signals: is FGF21 a nutritional adaptation factor?, *PLoS One*. 6 (2011) e22976.
- [53] G. Filhoulaud, S. Guilmeau, R. Dentin, J. Girard, C. Postic, Novel insights into ChREBP regulation and function, *Trends Endocrinol. Metab. TEM*. 24 (2013) 257–268.
- [54] R. Dentin, L. Tomas-Cobos, F. Fougelle, J. Leopold, J. Girard, C. Postic, et al., Glucose 6-phosphate, rather than xylulose 5-phosphate, is required for the activation of ChREBP in response to glucose in the liver, *J. Hepatol.* 56 (2012) 199–209.
- [55] M.A. Herman, O.D. Peroni, J. Villoria, M.R. Schön, N.A. Abumrad, M. Blüher, et al., A novel ChREBP isoform in adipose tissue regulates systemic glucose metabolism, *Nature*. 484 (2012) 333–338.
- [56] U. Dressel, T.L. Allen, J.B. Pippal, P.R. Rohde, P. Lau, G.E.O. Muscat, The peroxisome proliferator-activated receptor beta/delta agonist, GW501516, regulates the expression of genes involved in lipid catabolism and energy uncoupling in skeletal muscle cells, *Mol. Endocrinol.* 17 (2003) 2477–2493.
- [57] T. Tanaka, J. Yamamoto, S. Iwasaki, H. Asaba, H. Hamura, Y. Ikeda, et al., Activation of peroxisome proliferator-activated receptor delta induces fatty acid beta-oxidation in skeletal

muscle and attenuates metabolic syndrome, *Proc. Natl. Acad. Sci. U. S. A.* 100 (2003) 15924–15929.

- 1
2
3
4 [58] Y.-X. Wang, C.-H. Lee, S. Tiep, R.T. Yu, J. Ham, H. Kang, et al., Peroxisome-proliferator-
5
6 activated receptor delta activates fat metabolism to prevent obesity, *Cell.* 113 (2003) 159–170.
7
8 [59] G.I. Shulman, Cellular mechanisms of insulin resistance, *J. Clin. Invest.* 106 (2000) 171–176.
9
10 [60] E.B. Taylor, D. An, H.F. Kramer, H. Yu, N.L. Fujii, K.S.C. Roeckl, et al., Discovery of
11
12 TBC1D1 as an insulin-, AICAR-, and contraction-stimulated signaling nexus in mouse
13
14 skeletal muscle, *J. Biol. Chem.* 283 (2008) 9787–9796.
15
16 [61] X. Xi, J. Han, J.Z. Zhang, Stimulation of glucose transport by AMP-activated protein kinase
17
18 via activation of p38 mitogen-activated protein kinase, *J. Biol. Chem.* 276 (2001) 41029–
19
20 41034.
21
22 [62] G. Mithieux, L. Guignot, J.-C. Bordet, N. Wiernsperger, Intrahepatic mechanisms underlying
23
24 the effect of metformin in decreasing basal glucose production in rats fed a high-fat diet,
25
26 *Diabetes.* 51 (2002) 139–143.
27
28 [63] N. Musi, M.F. Hirshman, J. Nygren, M. Svanfeldt, P. Bavenholm, O. Rooyackers, et al.,
29
30 Metformin increases AMP-activated protein kinase activity in skeletal muscle of subjects with
31
32 type 2 diabetes, *Diabetes.* 51 (2002) 2074–2081.
33
34 [64] G. Mithieux, Metformin and the gut function, in: *Metformin Mech. Insights New Appl.*,
35
36 Transworld Research Network, Kerala, India, 2008: pp. 31–40.
37
38 [65] A. Grefhorst, M. Schreurs, M.H. Oosterveer, V.A. Cortés, R. Havinga, A.W. Herling, et al.,
39
40 Carbohydrate-response-element-binding protein (ChREBP) and not the liver X receptor α
41
42 (LXR α) mediates elevated hepatic lipogenic gene expression in a mouse model of glycogen
43
44 storage disease type 1, *Biochem. J.* 432 (2010) 249–254.
45
46 [66] Z. Sun, M.A. Lazar, Dissociating fatty liver and diabetes, *Trends Endocrinol. Metab. TEM.* 24
47
48 (2013) 4–12.
49
50
51
52
53
54
55
56
57
58
59
60
61
62
63
64
65

- 1
2
3
4
5
6
7
8
9
10
11
12
13
14
15
16
17
18
19
20
21
22
23
24
25
26
27
28
29
30
31
32
33
34
35
36
37
38
39
40
41
42
43
44
45
46
47
48
49
50
51
52
53
54
55
56
57
58
59
60
61
62
63
64
65
- [67] Z. Sun, R.A. Miller, R.T. Patel, J. Chen, R. Dhir, H. Wang, et al., Hepatic Hdac3 promotes gluconeogenesis by repressing lipid synthesis and sequestration, *Nat. Med.* 18 (2012) 934–942.
- [68] F.M. Fisher, S. Kleiner, N. Douris, E.C. Fox, R.J. Mepani, F. Verdeguer, et al., FGF21 regulates PGC-1 α and browning of white adipose tissues in adaptive thermogenesis, *Genes Dev.* 26 (2012) 271–281.
- [69] X. Ge, C. Chen, X. Hui, Y. Wang, K.S.L. Lam, A. Xu, Fibroblast growth factor 21 induces glucose transporter-1 expression through activation of the serum response factor/Ets-like protein-1 in adipocytes, *J. Biol. Chem.* 286 (2011) 34533–34541.
- [70] A. Kharitonov, A.C. Adams, Inventing new medicines: The FGF21 story, *Mol. Metab.* 3 (2014) 221–229.
- [71] G. Gaich, J.Y. Chien, H. Fu, L.C. Glass, M.A. Deeg, W.L. Holland, et al., The effects of LY2405319, an FGF21 analog, in obese human subjects with type 2 diabetes, *Cell Metab.* 18 (2013) 333–340.
- [72] J. Huang, T. Ishino, G. Chen, P. Rolzin, T.F. Osothprarop, K. Retting, et al., Development of a novel long-acting antidiabetic FGF21 mimetic by targeted conjugation to a scaffold antibody, *J. Pharmacol. Exp. Ther.* 346 (2013) 270–280.
- [73] T.D. Müller, L.M. Sullivan, K. Habegger, C.-X. Yi, D. Kabra, E. Grant, et al., Restoration of leptin responsiveness in diet-induced obese mice using an optimized leptin analog in combination with exendin-4 or FGF21, *J. Pept. Sci. Off. Publ. Eur. Pept. Soc.* 18 (2012) 383–393.
- [74] M.H. Tschöp, R.D. DiMarchi, Outstanding Scientific Achievement Award Lecture 2011: defeating diabetes: the case for personalized combinatorial therapies, *Diabetes.* 61 (2012) 1309–1314.

1
2
3
4
5
6
7
8
9
10
11
12
13
14
15
16
17
18
19
20
21
22
23
24
25
26
27
28
29
30
31
32
33
34
35
36
37
38
39
40
41
42
43
44
45
46
47
48
49
50
51
52
53
54
55
56
57
58
59
60
61
62
63
64
65

A link between hepatic glucose production and peripheral energy metabolism via hepatokines

FIGURE CAPTIONS

Figure 1. Protection from diabetes in L-G6pc^{-/-} mice fed a high fat/high sucrose diet.

(a) Loss of G6Pase activity and G6PC expression in L-G6pc^{-/-} mice (black symbols) detected by western blot compared to wild-type mice (+/+) (open symbols). (b) Hepatic G6P content in 6h-fasted mice. (c) Hepatic glycogen content in fed and 6h-fasted mice. (d) Plasmatic glucagon level in fed state. (e) Blood glucose and insulin levels during a glucose tolerance test in fed mice. (f) Blood glucose changes during an insulin tolerance test in fed mice. (g) 2-deoxyglucose uptake in BAT, subcutaneous WAT, epididymal WAT and the long digital extensor muscle (LDE) in basal state. (h) Blood glucose in 16h-fasted mice. Data are mean ± s.e.m. *P<0.05, **P<0.01, between L-G6pc^{-/-} mice and wild-type (+/+) mice. [§]p<0.05, between before and after glucose injection. Male mice were used after 21 weeks on HF/HS diet, except for glucose and insulin tolerance tests, which were performed after 12 weeks on HF/HS diet.

Figure 2. Protection from obesity in L-G6pc^{-/-} mice fed a high fat/high sucrose diet.

(a) **Photograph of representative** L-G6pc^{-/-} and wild-type mice fed a HF/HS diet. (b) Body weight changes of L-G6pc^{-/-} (black symbols) and wild-type mice (+/+) (open symbols). (c) Food intake of mice. (d) Body fat percentage. (e) Gonadal, subcutaneous and visceral fat weight/body weight. (f) Blood leptin and adiponectin levels. Data are mean ± s.e.m. *P<0.05, **P<0.01, between L-G6pc^{-/-} mice and wild-type (+/+) mice. Male mice were analyzed after 21 weeks on HF/HS diet.

Figure 3. Increased energy expenditure, thermogenesis and β -oxidation in L-G6pc^{-/-} mice fed a high fat/high sucrose diet.

(a) Spontaneous motor activity during 24 hours, (b) Energy expenditure (EE), (c) Whole-body oxygen consumption (VO₂), and (d) Rectal temperature of L-G6pc^{-/-} (black bars) and wild/type (+/+) (open bars) mice. (e) **Blood free fatty acid (FFA) level in 6h-fasted mice.** (f) Expression of genes associated with energy expenditure in muscle of L-G6pc^{-/-} mice relative to wild-type (100%). *Ppar*, Proliferator-activated receptor, *Ppargc1a*, PPAR-coactivator 1 α , *Ucp*, uncoupling protein, *cox4*, cytochrome c oxidase subunit IV, *Cytcs*, cytochrome c, *Cd36*, CD36 antigen, *Lpl*, lipoprotein lipase, *Acox1*, acyl-Coenzyme A oxidase 1, *Cpt1b*, carnitine palmitoyltransferase 1b. (g) Respiration rates (expressed as nmol O/min/mg protein) of mitochondria isolated from muscles in the presence of pyruvate/malate (state 4). Phosphorylating respiration (state 3) was initiated with 500 μ M ADP. Non phosphorylating respiration (state 4) was obtained by addition of oligomycin and fully uncoupled respiration was obtained with 2 μ M FCCP. Respiration rate associated with cytochrome c oxidase (COX) activity was measured after addition of ascorbate/TMPD. (h) Western blot analyses of phosphorylated and total AMPK, AMP-activated protein, phosphorylated and total ACC, acetyl-coenzyme A carboxylase, and phosphorylated and total MAPK, p38 mitogen-activated protein kinase in muscle. (i) Succinic dehydrogenase (SDH) staining of gastrocnemius fibers. **The quantification of oxidative (type I+type IIa) and glycolytic fibers was performed on three slides of both L-G6pc^{-/-} mice and wild-type mice and results are expressed in percent of total counted fibers. Bars represent 500 μ m** (j) Western blot analyses of Myosin Heavy Chain Type 1 and β -actin. Data are mean \pm s.e.m. *P<0.05, **P<0.01, between L-G6pc^{-/-} mice and wild-type mice. Male mice were analyzed after 21 weeks on HF/HS diet.

Figure 4. Increased thermogenesis in L-G6pc^{-/-} mice fed a high fat/high sucrose diet.

Expression of genes associated with energy expenditure in BAT (a) and WAT (b) of L-G6pc^{-/-} mice (black bars) relative to wild-type (open bars). *Cytcs*, cytochrome c, *Cox4*, cytochrome c oxidase subunit IV, *Ppar*, Proliferator-activated receptor, *Ppargc1a*, PPAR-coactivator 1 α , *Prdm16*, PR domain containing 16, *Ucp*, uncoupling protein, *Hsl*, hormone-sensitive lipase, *Atgl*, adipose triglyceride lipase. Histological analyses of BAT and WAT by H&E staining. Bars represent 100 μ m. Data are expressed as mean \pm s.e.m. *P<0.05, **P<0.01, between L-G6pc^{-/-} mice and wild-type (+/+) mice. Male mice were analyzed after 21 weeks on HF/HS diet.

Figure 5. Role of hepatokines in the phenotype of L-G6pc^{-/-} mice

(a) Relative mRNA level of hepatic regulators of glucose metabolism: *Fgf21*, fibroblast growth factor 21, *Agf*, Angiopoietin-related growth factor, *Angptl4*, angiopoietin-like 4, *Angptl3*, angiopoietin-like 3, *Hgf*, hepatocyte growth factor, *Igf1*, insulin-like growth factor 1, Adropin (Enho), Selenoprotein P (SeP) and fetuin in the liver of fed L-G6pc^{-/-} mice (black bars) or wild-type (open bars) mice. (b-c) Plasmatic level of FGF21 and AGF. (d-e) Blood glucose during a glucose tolerance test (d) and an insulin tolerance test (e) in L-G6pc^{-/-} (black circle), FGF21^{-/-}.L-G6pc^{-/-} (black square) and wild-type (open circle) mice. (f-g) Body weight and gonadal and subcutaneous WAT weight (% of body weight) of L-G6pc^{-/-} (black bars), FGF21^{-/-}.L-G6pc^{-/-} (hatched bars) and wild-type (white bars) mice. (h) Relative expression of UCP1 compared to β tubulin analyzed by western blot. (i) Expression of total ChREBP analyzed by western blot (top panel) and relative expression of ChREBP isoforms analyzed by RT-qPCR. Results are mean \pm s.e.m. *P<0.05, **P<0.01, between L-G6pc^{-/-} mice and wild-type mice (+/+). ^{\$}P<0.05, between L-G6pc^{-/-} mice and FGF21^{-/-}.L-G6pc^{-/-}. Male mice were analyzed after 21 weeks on HF/HS diet.

Figure 6. Suppression of hepatic glucose production reverses diabetes and increases energy expenditure in diabetic mice.

(a) Blood glucose in 16h-fasted mice before (L-G6pc^{lox/lox}, grey symbols) or 10 days after tamoxifen treatment of L-G6pc^{lox/lox} mice (od.L-G6pc^{-/-}, black symbols). (b) Plasmatic insulin level in 6h-fasted mice before or after tamoxifen treatment. (c-d) Blood glucose changes after glucose (c) or insulin (d) injection in fed mice before or 10 days (c) or 3 weeks (d) after tamoxifen treatment. (e) Weight body changes of floxed *G6pc* mice (G6Pc^{lox/lox}, grey symbols), floxed *G6pc* mice after tamoxifen treatment (od.L-G6pc^{-/-} mice, black symbols) and control mice (+/+, white symbols). (f-g) WAT weight and leptin levels 14 weeks after the tamoxifen treatment. (h-j) Relative mRNA expression of gene associated with energy expenditure in muscle (h), in BAT (i) and WAT (j) On panel h, western blot analysis of phosphorylated and total form of AMPK and P38MAPK in the muscle. **Quantification of western blot showed a 2.4-fold induction of P-AMPK expression in L-G6pc^{-/-} mice compared to control mice. P38MAPK activation was not statistically different.** On panel j, histological analysis of WAT by H&E staining. Bars represent 100 μm. (k) Relative hepatic mRNA content of hepatokines and plasmatic level of FGF21. **On the right of panel k, histological analysis of livers by H&E staining. Bars represent 100 μm.** Results are means ± s.e.m. *P<0.05, **P<0.01, between ob.L-G6pc^{-/-} and G6pc^{lox/lox} mice (panels a-e) and between ob.L-G6pc^{-/-} and control mice (panels e-k).

Figure 1

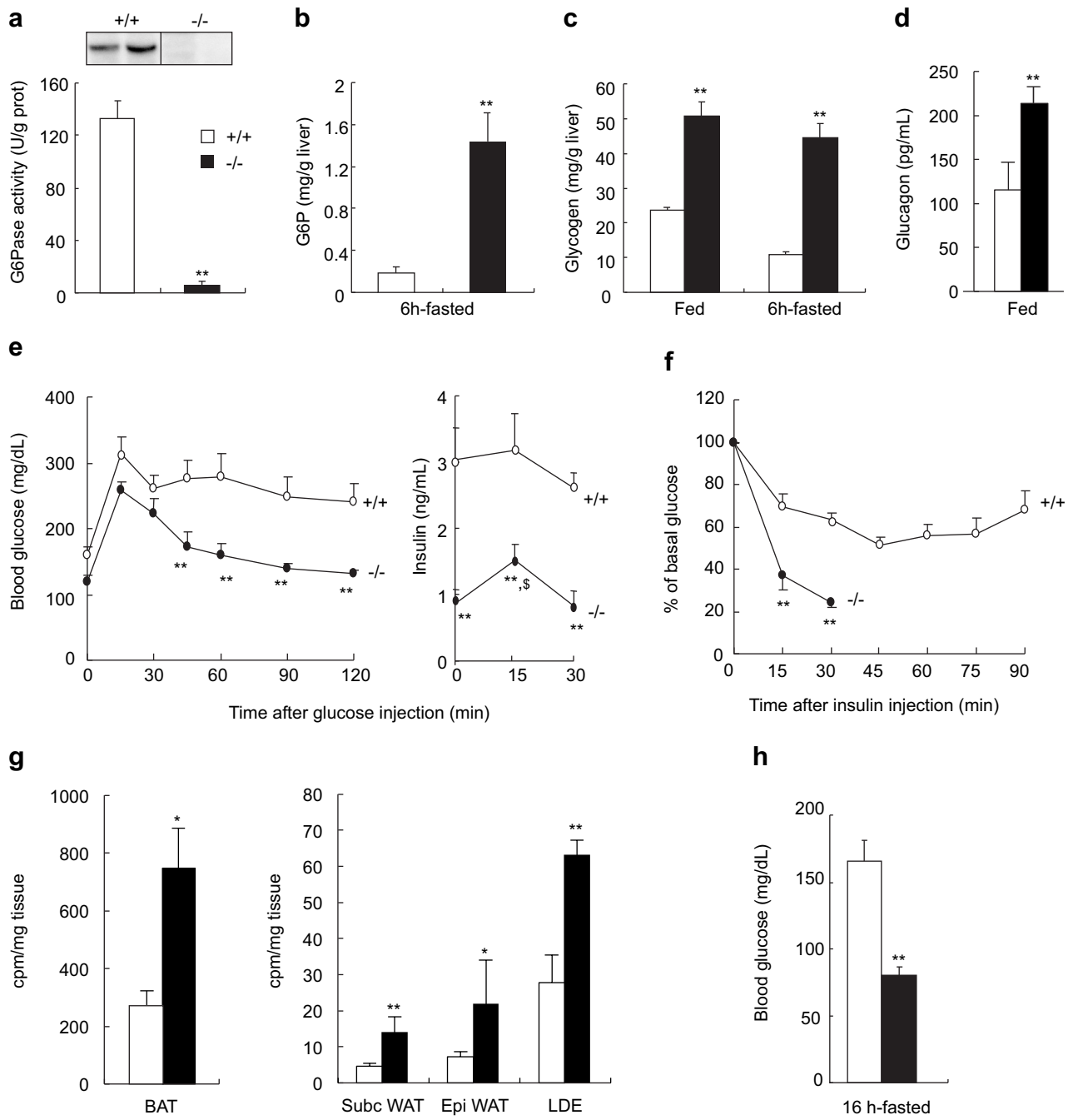


Figure 1, Abdul-Wahed et al.

Figure 2

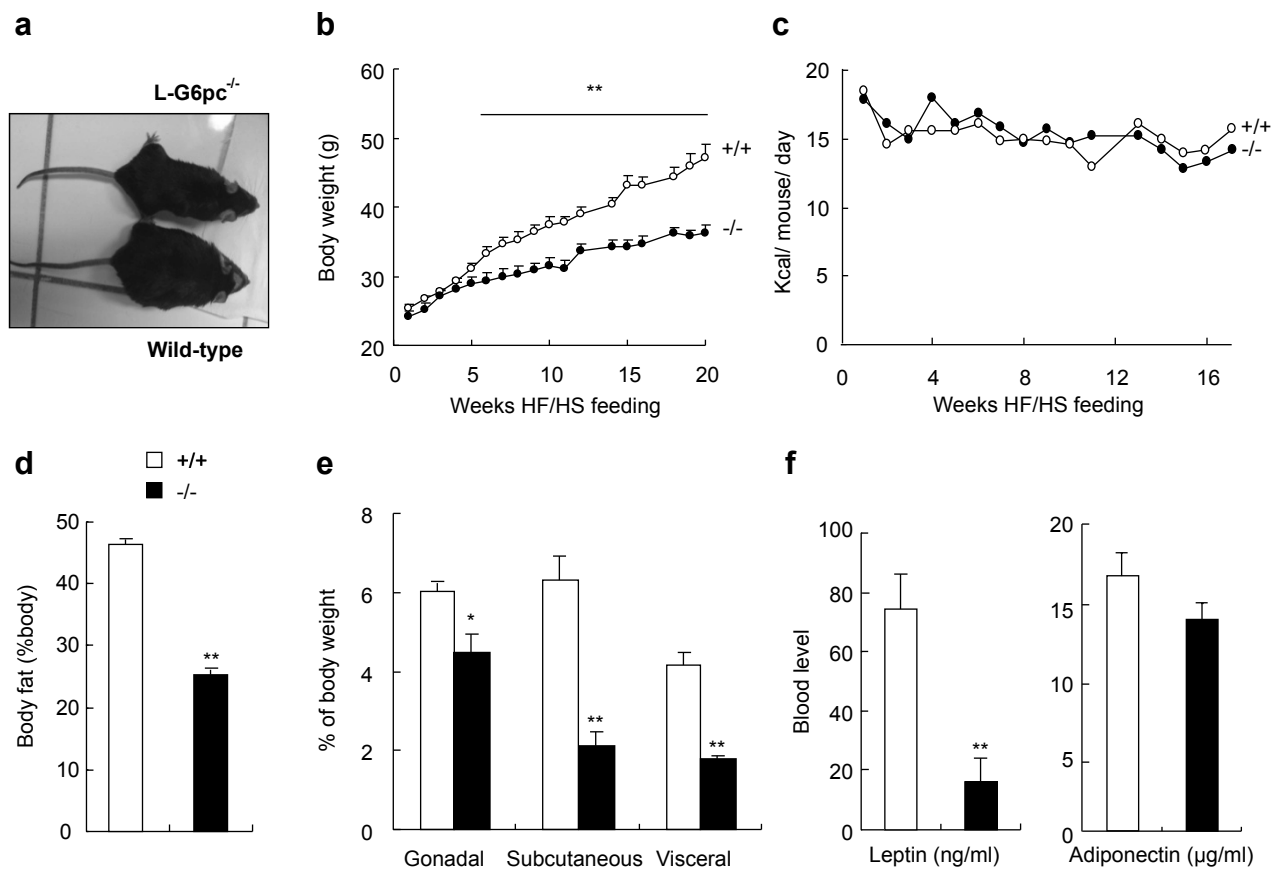


Figure 2, Abdul-Wahed et al.

Figure 3

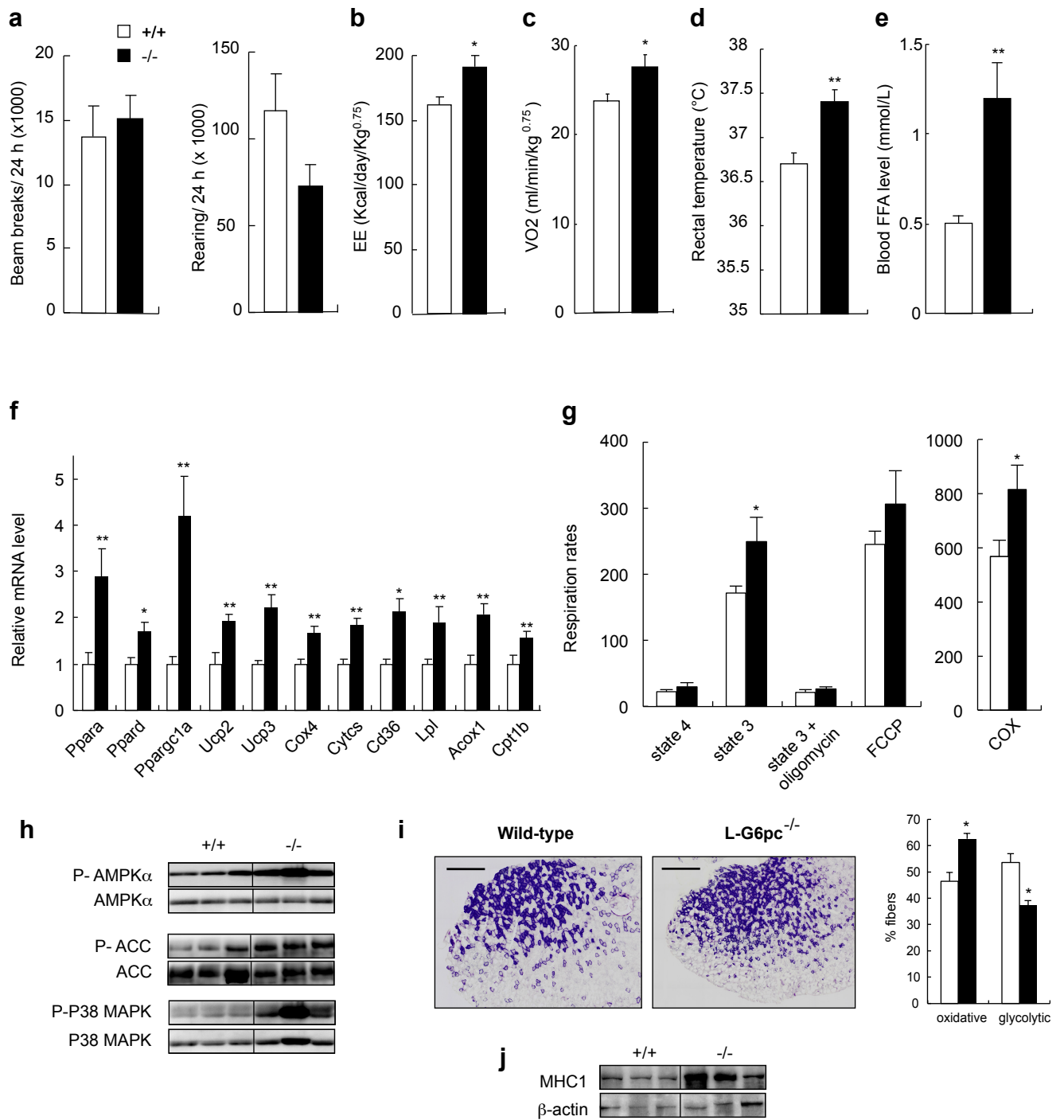


Figure 3, Abdul-Wahed et al. (color reproduction on the Web and in print)

Figure 4

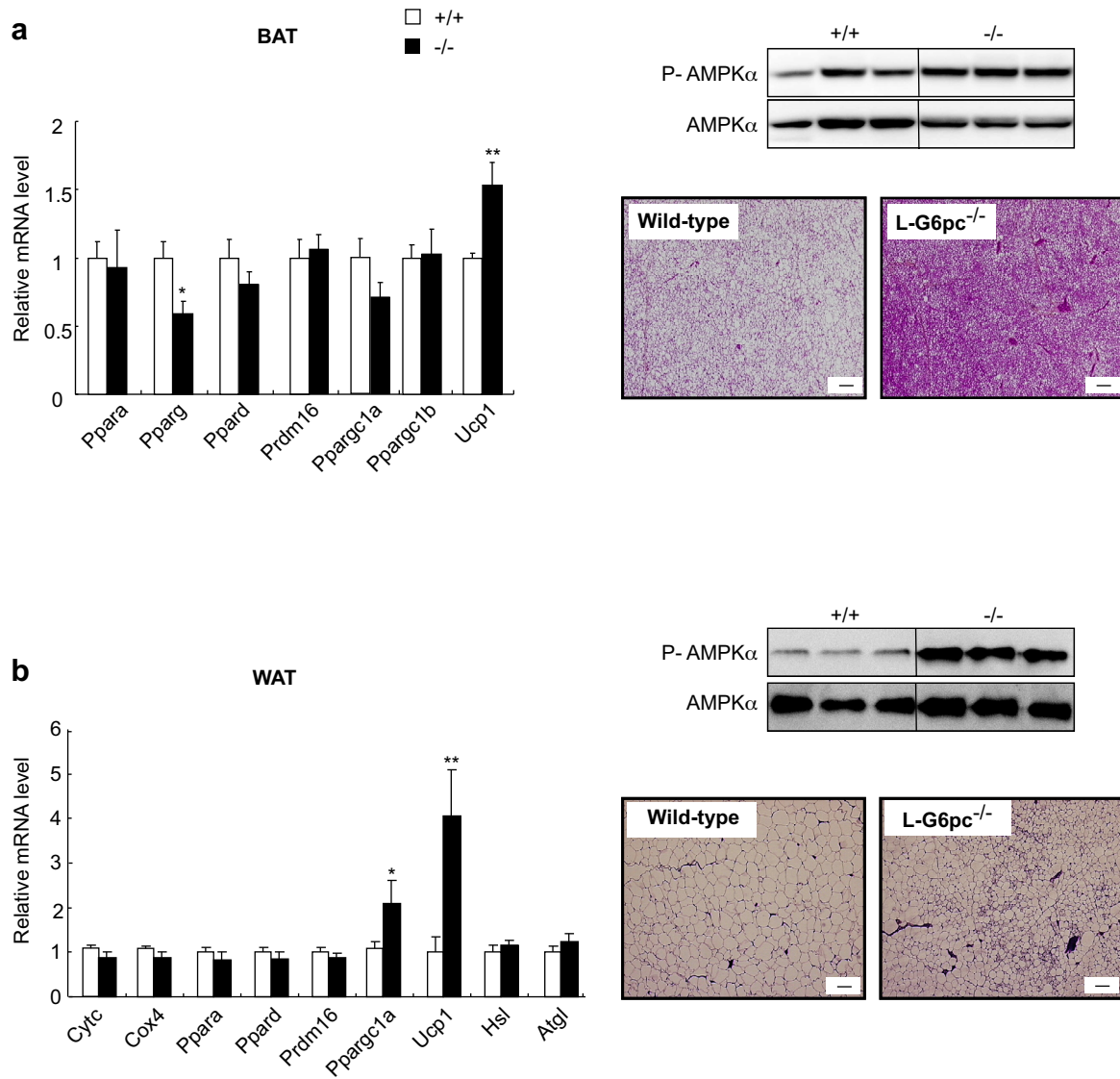


Figure 4, Abdul-Wahed et al. (color reproduction on the Web and in print)

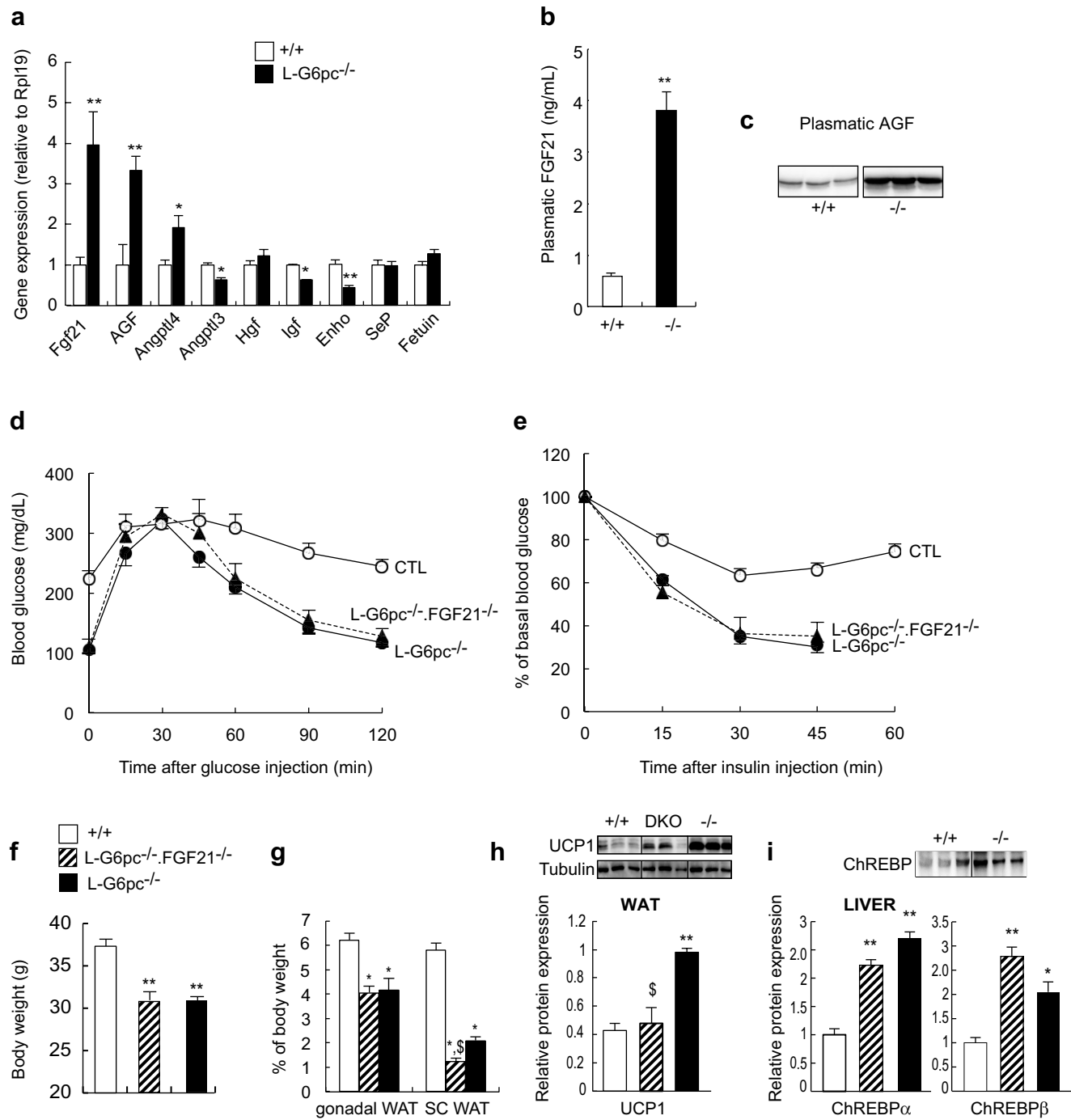


Figure 5, Abdul-Wahed et al.

Figure 6

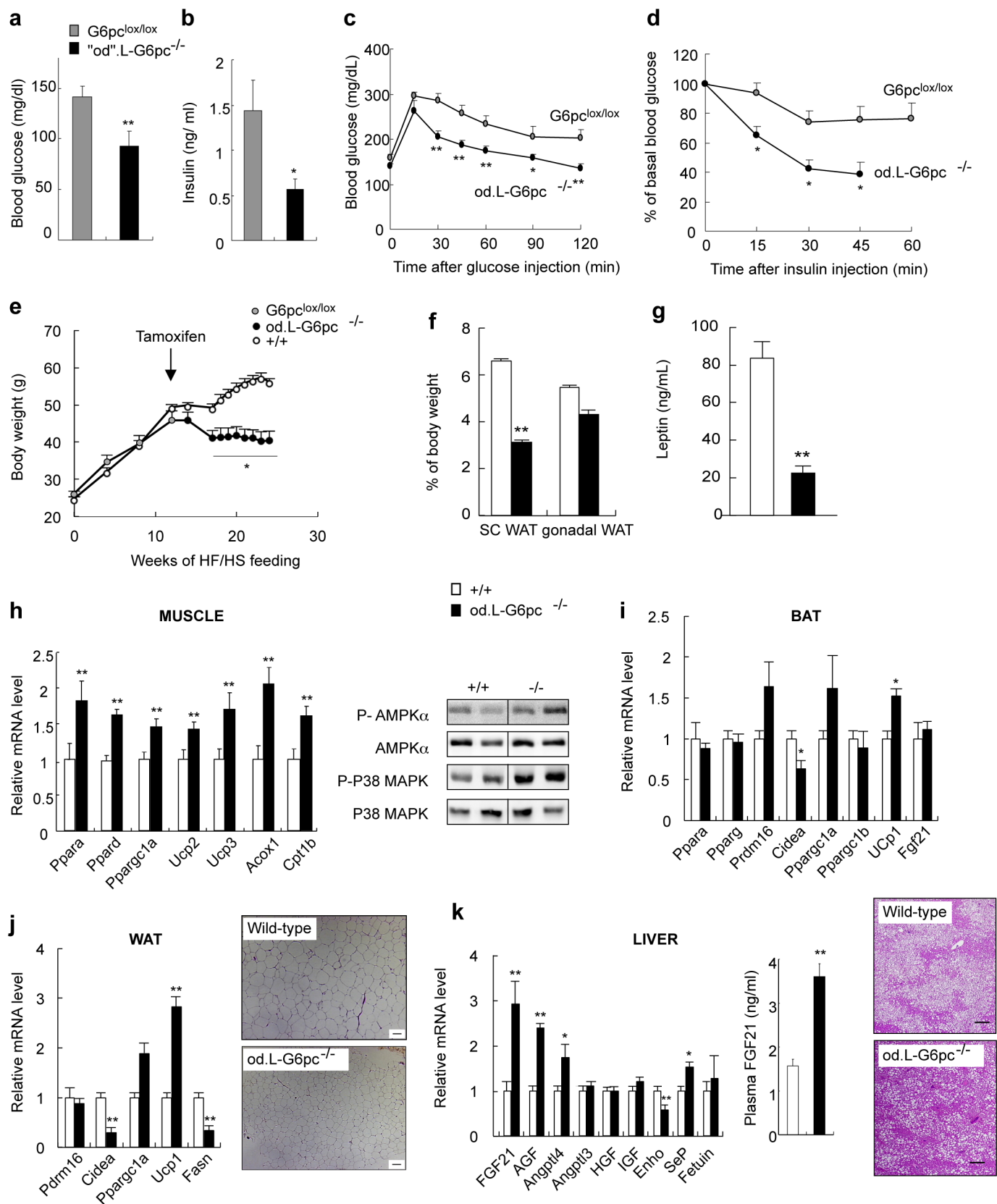


Figure 6, Abdul-Wahed et al.